

Are your MRI contrast agents cost-effective?

Learn more about generic Gadolinium-Based Contrast Agents.



FRESENIUS  
KABI

caring for life

**AJNR**

**Diffusion-Weighted Imaging of the  
Cerebellum in the Fetus with Chiari II  
Malformation**

C. Mignone Philpott, P. Shannon, D. Chitayat, G. Ryan,  
C.A. Raybaud and S.I. Blaser

This information is current as  
of April 19, 2024.

*AJNR Am J Neuroradiol* 2013, 34 (8) 1656-1660

doi: <https://doi.org/10.3174/ajnr.A3468>

<http://www.ajnr.org/content/34/8/1656>

# Diffusion-Weighted Imaging of the Cerebellum in the Fetus with Chiari II Malformation

C. Mignone Philpott, P. Shannon, D. Chitayat, G. Ryan, C.A. Raybaud, and S.I. Blaser

## ABSTRACT

**BACKGROUND AND PURPOSE:** Diffusion-weighted imaging can be used to characterize brain maturation. MR imaging of the fetus is used in cases of suspected Chiari II malformation when further evaluation of the posterior fossa is required. We sought to investigate whether there were any quantitative ADC abnormalities of the cerebellum in fetuses with this malformation.

**MATERIALS AND METHODS:** Measurements from ROIs acquired in each cerebellar hemisphere and the pons were obtained from calculated ADC maps performed on our Avanto 1.5T imaging system. Values in groups of patients with Chiari II malformations were compared with those from fetuses with structurally normal brains, allowing for the dependent variable of GA by using linear regression analysis.

**RESULTS:** There were 8 fetuses with Chiari II malformations and 23 healthy fetuses, ranging from 20 to 31 GW. There was a significant linear decline in the cerebellar ADC values with advancing gestation in our healthy fetus group, as expected. The ADC values of the cerebellum of fetuses with Chiari II malformation were higher [ $1820 (\pm 100) \times 10^{-6} \text{ mm}^2/\text{s}$ ] than ADC values in the healthy fetuses [ $1370 \pm 70) \times 10^{-6} \text{ mm}^2/\text{s}$ ]. This was statistically significant, even when allowing for the dependent variable of GA ( $P = .0126$ ). There was no significant difference between the pons ADC values in these groups ( $P = .645$ ).

**CONCLUSIONS:** While abnormal white matter organization or early cerebellar degeneration could potentially contribute to our findings, the most plausible explanation pertains to abnormalities of CSF drainage in the posterior fossa, with increased extracellular water possibly accounting for this phenomenon.

**ABBREVIATIONS:** FA = fractional anisotropy; GA = gestational age; GW = weeks' gestation; HASTE = half-Fourier acquired single-shot turbo spin-echo

Diffusion-weighted imaging can be used to characterize brain maturation in the fetus and infant. The decline in ADC values with increasing gestational age is thought to reflect the reduction in total water content, rise in lipids, and increased cell membrane surface-to-volume ratio.<sup>1</sup> There is a negative linear decline in values in the fetal brain, with a logarithmic decline in the first

year of life and continued decline evident until 2 years of age.<sup>1,2</sup> The ADC values and rate of decline are dependent on the location in the brain<sup>1</sup>: the cerebellar values are lower than those of supratentorial structures.<sup>3</sup>

The Chiari II malformation results from failure of closure of the caudal neuropore and subsequent failure of distention of the embryonic vesicles and mesenchymal stimulation necessary for normal posterior fossa growth and development, as proposed by the theory of McLone and Dias in 1989.<sup>4</sup> This small posterior fossa is unable to contain the developing cerebellum, which rapidly enlarges between 12 and 20 GW, and there is subsequent herniation of the vermis and hemispheres through the foramen magnum. This has since been confirmed with in vivo sheep studies, where Chiari II malformations resulted from myelotomies in the developing fetus, which were then reversed surgically.<sup>5</sup> In humans, intrauterine fetal repair of the myelomeningocele has also been shown to result in reversal of the Chiari II malformation<sup>6</sup> and is now considered a treatment option.

Received August 18, 2012; accepted after revision October 31.

From the Division of Neuroradiology (C.M.P., C.A.R., S.I.B.), Department of Diagnostic Imaging, Hospital for Sick Children, and Departments of Pathology (P.S.) and Prenatal Diagnosis and Medical Genetics (D.C.) and Fetal Medicine Unit (G.R.), Mount Sinai Hospital, University of Toronto, Toronto, Ontario, Canada.

Paper previously presented as "Pediatrics and Congenital Malformations," paper 0-134 at: Annual Meeting of the American Society of Neuroradiology and the Foundation of the ASNR Symposium, April 21-26, 2012; New York, New York.

Please address correspondence to Cristina Mignone Philpott, MD, Division of Neuroradiology, Department of Diagnostic Imaging, Hospital for Sick Children, University of Toronto, Toronto, Ontario M5G 1X8; e-mail: cristina.philpott@sickkids.ca

<http://dx.doi.org/10.3174/ajnr.A3468>

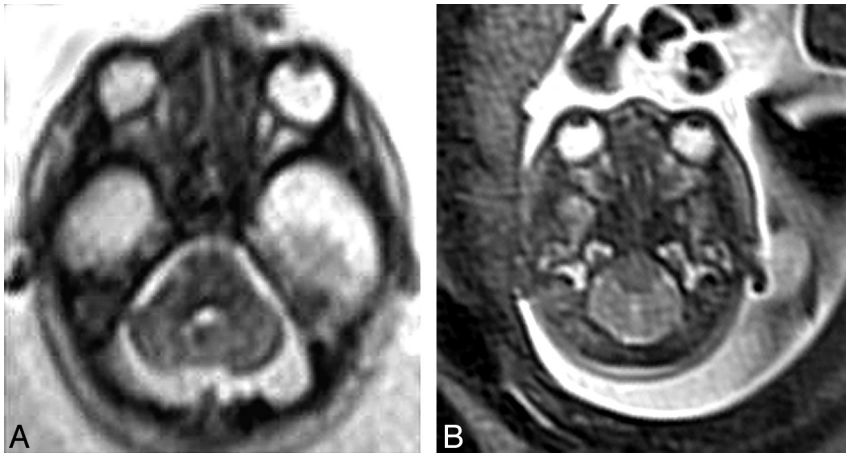


**FIG 1.** A, Axial HASTE image (TR = 2800, TE = 721, 4-mm section thickness) demonstrates high T2 signal in the cerebellar hemispheres at the level of the pons in a fetus with Chiari II malformation. B, Axial HASTE image (TR = 2800, TE = 721, 4-mm section thickness) demonstrates normal appearance of cerebellum in a fetus of the same gestational age (22 weeks).

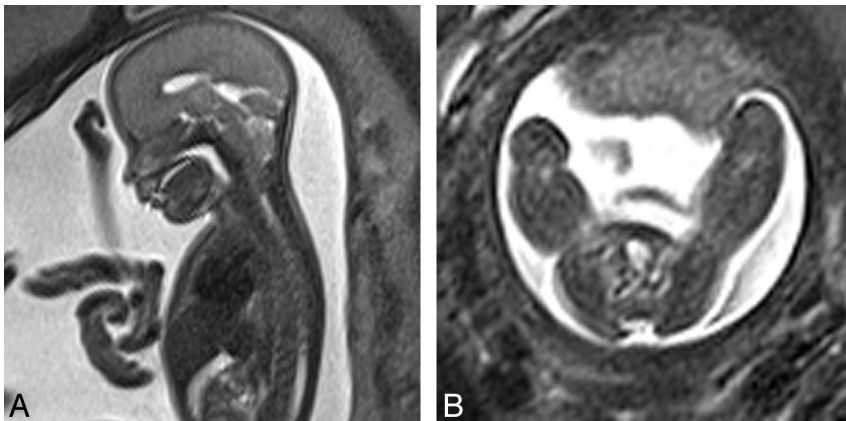


**FIG 2.** A, Sagittal HASTE image (TR = 2800, TE = 721, 4-mm section thickness) demonstrates a small posterior fossa and herniation of cerebellar tonsils through the foramen magnum in a fetus of 22 weeks' gestation. B, Axial HASTE image (TR = 2800, TE = 721, 4-mm section thickness) demonstrates a myelomeningocele in a fetus of 22 weeks' gestation.

Given abnormal posterior fossa development in the Chiari II malformation and observations of brighter cerebellar tissue on T2 and DWI (in fetuses of 19–21 weeks GA) (Fig 1A, -B), we were interested in further investigating differences in ADC values, which may reflect altered neuronal development.

### MATERIALS AND METHODS

We identified subjects by reviewing the formal reports and sequence records stored on our PACS system of all fetal MR imaging studies performed at our institution from January 2008 through March 2012. The images of fetuses in whom a Chiari II diagnosis was recorded were retrospectively reviewed. Those fetuses who demonstrated all 3 features of a Chiari II malformation were included in the patient group. These features were the following: a small posterior fossa, cerebellar tonsils herniating below the foramen magnum, and a myelomeningocele (Fig 2A, -B). Those who had no significant findings recorded were also reviewed for assessment of any cranial abnormalities, syndromal markers, and the presence of any extracranial malformations. Those fetuses who did not exhibit any of these abnormalities were included in the healthy control group. The indication for fetal imaging in all sub-

jects was recorded. Gestational age, ventricular size, and any associated abnormalities (in the patients with Chiari II) were also recorded.

Ethics approval from our institutional review board was obtained.

All fetal DWI had been acquired on a 1.5T imaging system (Avanto; Siemens, Erlangen, Germany), with a single-shot spin-echo echo-planar DWI sequence in the axial plane with  $b=0, 500, \text{ and } 1000 \text{ s/mm}^3$  in 3 orthogonal directions, by using a phased array abdominal coil. Axial, sagittal, and coronal plane HASTE; coronal T1 fast low-angle shot (gradient-echo sequence); and axial T2 gradient-echo sequences were also performed as part of the routine examination (parameters are outlined in the Table).

Averaged ADC maps were automatically performed by the Siemens software, and data were transferred to our local Advantage Workstation (GE Healthcare, Milwaukee, Wisconsin). Each image was reviewed by a pediatric neuroradiologist for the presence of motion or other artifacts, such as maternal bowel gas. Data were not obtained in sections affected by artifacts. Fetuses in whom there were too many motion artifacts to accurately measure the ROI were not included in the analysis.

Circular ROIs were drawn on the ADC maps in the right and left cerebellar hemispheres and pons, and values were recorded (Fig 3). The ROIs ranged from  $6.9 \text{ to } 17.9 \text{ mm}^2$  and were placed

within the central part of the cerebellar hemisphere. Because the right and left cerebellar hemisphere values were not significantly different (Pearson correlation coefficient = 0.96), these values were averaged for analysis and studies in which only 1 value could be obtained were included in the analysis as a single value.

The mean ADC cerebellar and pons values of the Chiari II and healthy groups were plotted against gestational age. We evaluated the relationship between gestational age and ADC values and compared ADC values in both groups, accounting for gestational age, by using analysis of covariance. A  $P$  value of  $< .05$  was considered significant.

### RESULTS

There were 23 healthy fetuses who ranged from 21 to  $31^{+2}$  GW, with a median GA of 27 weeks. These included 7 sets of dichorionic diamniotic twin gestations, in 3 of which there had been death of the cotwin and in 4 of which the cotwin had ventriculomegaly or vermian hypoplasia. The other healthy fetuses were imaged to evaluate questionable ventricular prominence or asymmetric ventricles on sonography, and one, because of a fetal death

### Acquisition parameters for fetal MRI

Sequence	Plane	FOV (mm)	Matrix	Section Thickness (mm)	TR (ms)	TE (ms)	Signal Averages	Sections	Acquisition Time (min:sec)
DWI <sup>a</sup>	Axial	300 × 300	128 × 75	4	2800	721	4	12	00:24
HASTE	Axial	310 × 310	320 × 80	3.5	2043	166	0	15	00:19
HASTE	Coronal	310 × 310	320 × 80	3.5	2043	166	0	15	00:19
HASTE	Sagittal	310 × 310	320 × 80	3.5	2043	166	0	15	00:19
TI FLASH	Coronal	320 × 256	256 × 100	4	69	4.5	0	15	00:30
SWI	Axial	300 × 300	256 × 79	4	143	20	0	15	00:45

**Note:**—FLASH indicates fast low-angle shot.

<sup>a</sup> Single-shot spin-echo echo-planar,  $b=0, 500, 1000$ .

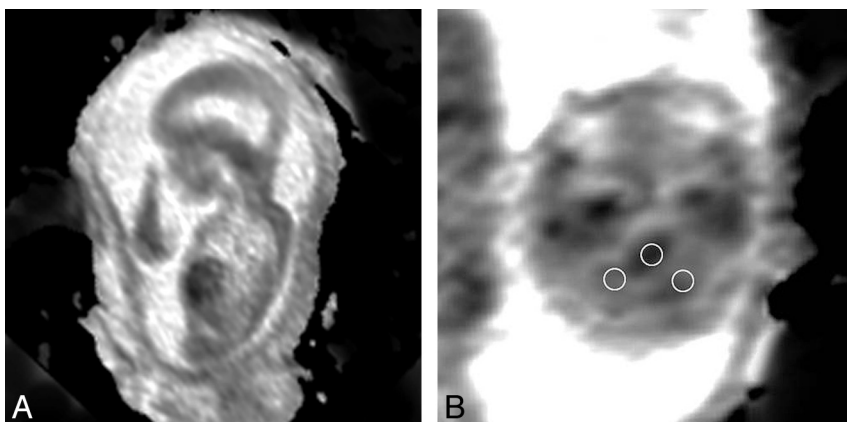


**FIG 3.** A, Sagittal ADC map (TR, 2800; TE, 721; 4-mm section thickness); B, Axial ADC map, (TR, 2800; TE, 721; 4-mm section thickness) demonstrates a region of interest placed over each cerebellar hemisphere and pons in a fetus with a Chiari II malformation.

in a previous pregnancy. There were 8 fetuses with Chiari II malformations who ranged in GA from 20 to 29 weeks (median, 22 weeks), all of whom had myelomeningoceles. We found a significant linear decline in cerebellar ADC values with advancing gestation in healthy fetuses ( $P < .0126$ ) (Fig 4). There was no relationship between gestational age and cerebellar ADC values in the Chiari II group ( $P = .24$ ).

The cerebellar ADC values in fetuses with Chiari II malformations were, on average, 35% higher [ $1820 (\pm 100) \times 10^{-6} \text{mm}^2/\text{s}$ ] than ADC values in the healthy fetuses ( $1370 \pm 70 \times 10^{-6} \text{mm}^2/\text{s}$ ). This was statistically significant, even allowing for the variation in gestational age ( $P = .0126$ ), as evident when plotting the average ADC values of both groups against gestation (Fig 4). The mean ADC value of the pons was higher in the Chiari II group versus the healthy group by  $1660 \times 10^{-6} \text{mm}^2/\text{s}$ , at any given gestation. However, this did not reach statistical significance ( $P = .645$ ) (Fig 5).

### DISCUSSION

We have found significant differences in cerebellar ADC values in fetuses with Chiari II malformations compared with the healthy fetuses, even taking into account the normal reduction in ADC values that occurs with advancing gestation. Indeed, the trend of cerebellar ADC values in fetuses with Chiari II malformations does not conform to a negative linear relationship, as it does in healthy fetuses.

Chiari II malformations are known to result from abnormal CSF pressures as a result of the open caudal neuropore, evident as the omnipresent myelomeningocele. The lack of normal neural vesicle distention during embryonic development results in inadequate and disorganized neural development and secondary ef-

fects on the growth of the surrounding mesenchyme.<sup>4</sup> The resultant small posterior fossa is unable to house the rapidly expanding hindbrain during midgestation, with subsequent herniation of the cerebellar tonsils, both superiorly through the tentorial incisura and inferiorly into the foramen magnum. The crowding of neural structures results in decreased CSF outflow and eventual hydrocephalus,<sup>7</sup> which further exacerbates the downward pressure on the herniating cerebellar tonsils.

With a series of DWI images with differing b-values, ADC maps can be calculated that depict the average rate of isotropic motion in each pixel, with higher values and correspondingly brighter signal reflecting stronger diffusion. Distribution of water in intra- and extracellular compartments, fiber and neuroglial cell attenuation, and transmembrane cellular proton movement are some of the factors that contribute to these ADC values.

There is a paucity of published data in regard to both ADC properties and fractional anisotropy of cerebellar structures in the Chiari II malformation. Reduced fractional anisotropy was shown in the middle cerebellar peduncles in a small cohort of young adults with Chiari II malformation, though no differences were demonstrated in the transverse pontine fibers or superior or inferior peduncles.<sup>8</sup> The authors proposed that given that the middle cerebellar peduncles convey prefrontal and precentral cortical motor fibers, the findings were likely due to altered cerebellar development rather than pressure effects because transverse pontine FA was not altered. This was described in the context of global abnormal neuronal development, including callosal dysgenesis, which has been described in the Chiari II malformation,<sup>4</sup> and was present in all their cases. Reduced FA and higher diffusivity have also been found in the major associative pathways of the supratentorial white matter tract in patients with Chiari II and are thought to reflect altered development and/or effects of chronic hydrocephalus on myelination, cell membrane integrity, and stretching of fibers.<sup>9,10</sup>

Therefore, our findings may indeed reflect altered neuronal cell or fiber packing or organization in the context of abnormal cerebellar development. Our findings are also consistent in that the ADC values of the pons were not significantly different from those in healthy controls. The transverse pontine fibers contribute to these ADC values, among others, which include cerebral cortical and ascending afferent fibers, which synapse with the pontine

### Cerebellar ADC values: Chiari 2 vs Normal

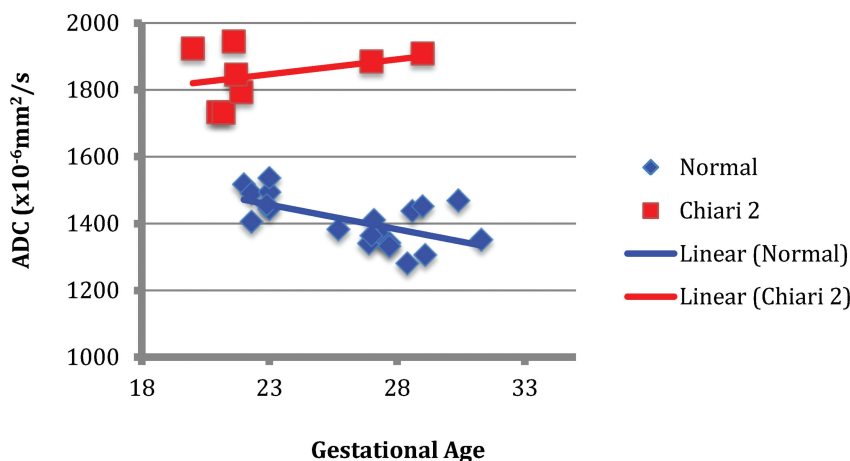


**FIG 4.** Chart demonstrating the higher cerebellar ADC values in the Chiari II group versus the healthy fetus group.

### Pons ADC values: Chiari 2 vs Normal

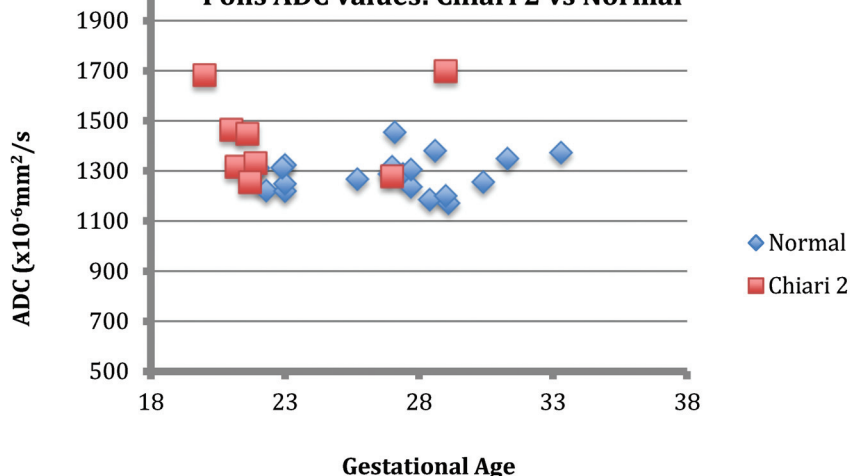


**FIG 5.** Chart demonstrating the pontine ADC values of the Chiari II group versus the healthy fetus group.

nuclei. However, because these postsynaptic transverse pontine fibers project into the middle cerebellar peduncles and deep cerebellar white matter,<sup>11</sup> one might also expect the pontine ADC values to also be altered in the context of abnormal cerebellar tract development. We did not find this to be the case.

Alternatively, our findings may directly or indirectly reflect altered CSF flow dynamics or chronic effects of increased CSF pressure on cell membrane integrity. Increases in ADC values have been found in periventricular white matter of hydrocephalic rats<sup>12</sup> and humans,<sup>13,14</sup> thought to be secondary to edema.<sup>15</sup> Therefore similar hydrostatic mechanisms, with obstruction of CSF outflow at the level of the foramen magnum in these fetuses, may result in increased extracellular water and hence elevated ADC values.

Early postmortem studies in infants and children have demonstrated reduced weight of the cerebellum in Chiari II malformation compared with controls.<sup>16</sup> These studies also demonstrated necrosis predominantly within the pyramid,

uvula, and nodule,<sup>17</sup> with a reduced number of granule cells also seen in the remnant tissue within these regions but also within the declive.<sup>18</sup> This necrosis was largely attributed to the direct pressure effects of the small posterior fossa. More recent volumetric studies have confirmed an overall reduction in cerebellar volume,<sup>19</sup> with the anterior lobe absolutely and relatively enlarged compared with absolute and relative reductions in the posterior lobe and corpus medullare volumes. Therefore, additional factors of altered membrane integrity and neuronal tissue composition (decreased cell membrane-to-extracellular fluid ratios), resulting from pressure effects, may also contribute to our findings.

The limitations of our study include the relatively small number of subjects, its retrospective nature, and unmatched controls. Data acquisition was difficult given the relatively small areas of cerebellum in the fetuses with Chiari II, though attempts were made to acquire data at the same levels through the pontine bellies and middle cerebellar peduncles.

### CONCLUSIONS

We found increased diffusivity in the cerebellum of fetuses with Chiari II malformations. This may reflect altered CSF hydrodynamics in the posterior fossa or the indirect effects of such dynamics on membrane and fiber composition. Follow-up assessment and investigation as to whether these findings can be used to predict postnatal prognosis may be

worthwhile, particularly if such information can help in patient selection for fetal therapy.

### ACKNOWLEDGMENT

We thank George Tomlinson, PhD, Assistant Professor Biostatistics, Department of Medicine, Department of Radiology, University of Toronto for performing statistical analyses.

Disclosures: Susan Blaser—UNRELATED: Royalties: Amirsys publication royalties, Comments: unrelated to this manuscript.

### REFERENCES

- Schneider JF, Confort-Gouny S, Le Fur Y, et al. Diffusion-weighted imaging in normal fetal brain maturation. *Eur Radiol* 2007;17:2422–29
- Lövblad KO, Schneider J, Ruoss K, et al. Isotropic apparent diffusion coefficient mapping of postnatal cerebral development. *Neuroradiology* 2003;45:400–03



3. Prayer D, Kasprian G, Krampl E, et al. **MRI of normal fetal brain development.** *Eur J Radiol* 2006;57:199–216
4. McLone DG, Dias MS. **The Chiari II malformation: cause and impact.** *Childs Nerv Syst* 2003;19:540–50
5. Bouchard S, Davey MG, Rintoul NE, et al. **Correction of hindbrain herniation and anatomy of the vermis after in utero repair of myelomeningocele in sheep.** *J Pediatr Surg* 2003;38:451–58, discussion 51–58
6. Sutton LN, Adzick NS, Bilaniuk LT, et al. **Improvement in hindbrain herniation demonstrated by serial fetal magnetic resonance imaging following fetal surgery for myelomeningocele.** *JAMA* 1999;282:1826–31
7. Stein SC, Schut L. **Hydrocephalus in myelomeningocele.** *Childs Brain* 1979;5:413–19
8. Herweh C, Akbar M, Wengenroth M, et al. **Reduced anisotropy in the middle cerebellar peduncle in Chiari-II malformation.** *Cerebellum* 2010;9:303–09
9. Hasan KM, Eluvathingal TJ, Kramer LA, et al. **White matter microstructural abnormalities in children with spina bifida myelomeningocele and hydrocephalus: a diffusion tensor tractography study of the association pathways.** *J Magn Reson Imaging* 2008;27:700–09
10. Ou X, Glasier CM, Snow JH. **Diffusion tensor imaging evaluation of white matter in adolescents with myelomeningocele and Chiari II malformation.** *Pediatr Radiol* 2011;41:1407–15
11. Wakana S, Jiang H, Nagae-Poetscher LM, et al. **Fiber tract-based atlas of human white matter anatomy.** *Radiology* 2004;230:77–87
12. Massicotte EM, Buist R, Del Bigio MR. **Altered diffusion and perfusion in hydrocephalic rat brain: a magnetic resonance imaging analysis.** *J Neurosurg* 2000;92:442–47
13. Gideon P, Thomsen C, Gjerris F, et al. **Increased self-diffusion of brain water in hydrocephalus measured by MR imaging.** *Acta Radiol* 1994;35:514–19
14. Leliefeld PH, Gooskens RH, Braun KP, et al. **Longitudinal diffusion-weighted imaging in infants with hydrocephalus: decrease in tissue water diffusion after cerebrospinal fluid diversion.** *J Neurosurg Pediatr* 2009;4:56–63
15. Tamaki N, Yamashita H, Kimura M, et al. **Changes in the components and content of biological water in the brain of experimental hydrocephalic rabbits.** *J Neurosurg* 1990;73:274–78
16. Variend S, Emery JL. **The weight of the cerebellum in children with myelomeningocele.** *Dev Med Child Neurol Suppl* 1973;(suppl 29):77–83
17. Variend S, Emery JL. **The pathology of the central lobes of the cerebellum in children with myelomeningocele.** *Dev Med Child Neurol* 1974;16:99–106
18. Emery JL, Gadsdon DR. **A quantitative study of the cell population of the cerebellum in children with myelomeningocele.** *Dev Med Child Neurol Suppl* 1975:20–25
19. Fletcher JM, Copeland K, Frederick JA, et al. **Spinal lesion level in spina bifida: a source of neural and cognitive heterogeneity.** *J Neurosurg* 2005;102:268–79